An oxygen-sensing mechanism for angiosperm adaptation to altitude

https://doi.org/10.1038/s41586-022-04740-y

Received: 25 June 2021

Accepted: 7 April 2022

Published online: 1 June 2022

Open access

Check for updates

Mohamad Abbas[1], Gunjan Sharma[1], Charlene Dambire[1], Julietta Marquez[1], Carlos Alonso-Blanco[2], Karina Proaño[3] & Michael J. Holdsworth[1]✉

Flowering plants (angiosperms) can grow at extreme altitudes, and have been observed growing as high as 6,400 metres above sea level[1,2]; however, the molecular mechanisms that enable plant adaptation specifically to altitude are unknown. One distinguishing feature of increasing altitude is a reduction in the partial pressure of oxygen (pO_2). Here we investigated the relationship between altitude and oxygen sensing in relation to chlorophyll biosynthesis—which requires molecular oxygen[3]—and hypoxia-related gene expression. We show that in etiolated seedlings of angiosperm species, steady-state levels of the phototoxic chlorophyll precursor protochlorophyllide are influenced by sensing of atmospheric oxygen concentration. In *Arabidopsis thaliana*, this is mediated by the PLANT CYSTEINE OXIDASE (PCO) N-degron pathway substrates GROUP VII ETHYLENE RESPONSE FACTOR transcription factors (ERFVIIs). ERFVIIs positively regulate expression of *FLUORESCENT IN BLUE LIGHT* (*FLU*), which represses the first committed step of chlorophyll biosynthesis, forming an inactivation complex with tetrapyrrole synthesis enzymes that are negatively regulated by ERFVIIs, thereby suppressing protochlorophyllide. In natural populations representing diverse angiosperm clades, we find oxygen-dependent altitudinal clines for steady-state levels of protochlorophyllide, expression of inactivation complex components and hypoxia-related genes. Finally, *A. thaliana* accessions from contrasting altitudes display altitude-dependent ERFVII activity and accumulation. We thus identify a mechanism for genetic adaptation to absolute altitude through alteration of the sensitivity of the oxygen-sensing system.

Around 25% of the Earth's land surface, containing at least 30% of plant species diversity[4], is mountainous. Although the altitude at which an individual plant grows may never change, it is critical that individuals (and populations) are adapted to survive at that altitude, and this is an important component of plant ecology[4]. Altitude and latitude have been considered collectively to impart a syndrome of developmental and physiological characteristics linked mostly to climatic adaptation (including dwarfism, resistance to ultra-violet light, low temperature tolerance, flowering time and others[4,5]). However, no consistent trait has been associated with specific environmental components of altitude, such as pO_2, which might reveal mechanisms underlying direct altitudinal adaptation. Here we investigate the idea that adaptation to altitude involves direct sensing of oxygen concentration across altitudinal ranges. Mammalian adaptation to very high altitude involved mutation of components of the hypoxia-inducible factor (HIF) oxygen-sensing system[6–8] (which is mechanistically different to the plant oxygen-sensing pathway[9]), indicating the importance of matching metabolism with altitude. Oxygen sensing in plants through Met1–Cys2 ERFVII transcription factors is mediated by the PCO branch of the PROTEOLYSIS 6 (PRT6) N-degron pathway[10,11]. Following Met1 removal, the amino-terminal cysteine is oxidized by PCOs[12] using molecular O_2, arginylated by arginyl transferase[13] and recognized by the E3 ligase PRT6 for ubiquitin-mediated destruction (Fig. 1a).

We reasoned that plant biochemical pathways that require oxygen may be subject to evolutionary pressure in relation to altitude. Tetrapyrrole synthesis, which leads to chlorophyll, is dependent on ambient O_2 at several points (Extended Data Fig. 1a). Following germination, during etiolated growth in the dark, the chlorophyll biosynthesis intermediate protochlorophyllide (Pchlide) accumulates because angiosperms possess only a light-activated chloroplast enzyme for Pchlide reduction[14] (light-dependent NADPH-protochlorophyllide oxidoreductase (L-POR, hereafter POR)). We set out to determine whether differences in pO_2 with altitude could influence the flux through the tetrapyrrole pathway through oxygen sensing and be a target for evolutionary adaptation. We first investigated whether the ambient O_2 concentration regulates steady-state Pchlide levels in plant species representing diverse angiosperm clades, *A. thaliana* (rosid), *Solanum lycopersicum* (asterid), *Papaver somniferum* (basal dicot) and *Brachypodium distachyon* (monocot) (Fig. 1b). This showed that decreasing ambient O_2 levels from 27% (hyperoxia) to 5% (hypoxia) decrease Pchlide levels in etiolated seedlings. To show that this is not just the result of hypoxia-related flux restrained by O_2-requiring enzymes of the pathway we also analysed

[1]School of Biosciences, University of Nottingham, Nottingham, UK. [2]Centro Nacional de Biotecnología, Consejo Superior de Investigaciones Científicas, Madrid, Spain. [3]Laboratorio de Biotecnología Vegetal, Departamento de Ciencias de la Vida y la Agricultura, Universidad de las Fuerzas Armadas ESPE, Sangolquí, Ecuador. ✉e-mail: michael.holdsworth@nottingham.ac.uk

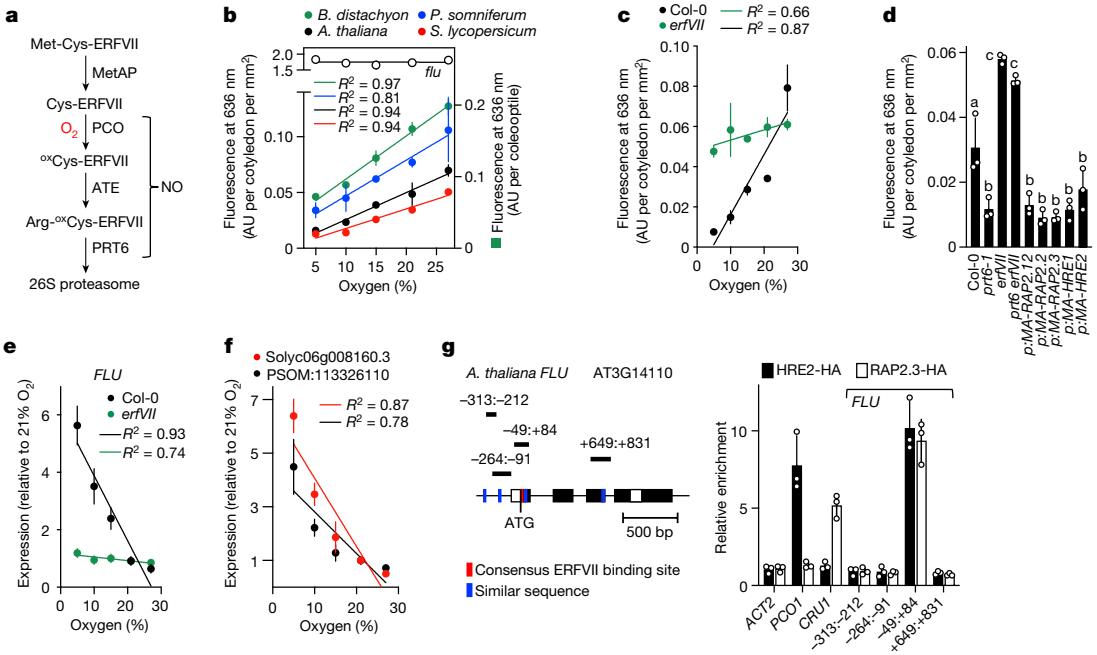

Fig. 1 | Atmospheric oxygen sensing regulates tetrapyrrole synthesis via FLU. a, Schematic representation of the PCO branch of the PRT6 N-degron pathway[28]. MetAP, methionine amino-peptidase; ATE, arginyl transferase; ^{ox}Cys, oxidized cysteine. The position of oxygen and possible positions of nitric oxide (NO) in the pathway are shown. Oxygen is used by PCOs to oxidize amino-terminal Cys of ERFVIIs. **b**, Steady-state Pchlide, measured by fluorescence at 636 nm, in etiolated seedlings of different species grown at different ambient O_2 concentrations. **c**, **d**, Steady-state Pchlide in Col-0 and *erfVII* at different ambient O_2 concentrations (**c**) with expression of individual stabilized Cys2Ala mutant ERFVIIs controlled by their native promoters (**d**)[18] (p). **e**, Amount of *FLU* RNA transcript in Col-0 and *erfVII* grown at different ambient O_2 concentrations. **f**, Regulation of *FLU* orthologue mRNA in *P. somniferum* (PSOM) and *S. lycopersicum* (Solyc) grown at various ambient O_2 concentrations. **g**, Schematic of the *A. thaliana FLU* gene, showing potential ERFVII binding sites (left) and chromatin immunoprecipitation (ChIP) analysis of RAP2.3–HA and HRE2–HA occupancy of *FLU* gene regions (range indicated by colons); including known positive and negative regulatory sequences[20,29] using anti-HA antibody. All experiments were carried out using etiolated seedlings after 5 days growth at pO_2 21.2 kPa (48 m a.s.l.) unless otherwise stated. Data are mean ± s.d.; one-way ANOVA. Significantly different groups are indicated by letters in **d**. $n = 3$ biologically independent experiments. AU, arbitrary units; R^2, coefficient of determination.

steady-state Pchlide levels for the *A. thaliana flu* mutant. FLU directly inhibits the first committed enzyme of tetrapyrrole synthesis, glutamyl tRNA reductase (GluTR)—the major form of which is encoded by *HEMA1*—thereby inhibiting synthesis of 5-aminolevulinic acid (ALA), the precursor of all tetrapyrroles[15], which results in prevention of accumulation of free Pchlide (Extended Data Fig. 1a). The proposed mechanism for FLU activity involves POR, Pchlide, GluTR and CHL27 (a component of the tetrapyrrole synthesis enzyme Mg-protoporphyrin monomethylester cyclase[3]); in the dark, free Pchlide (which cannot be converted to chlorophyllide without light) binds POR as part of a complex with CHL27 and FLU. This inactivation complex enables FLU to interact with and inhibit GluTR activity, reducing ALA synthesis and therefore Pchlide levels[16,17]. Under mild hypoxia, compared with normoxia and hyperoxia, steady-state Pchlide levels were unrestrained in the *flu* mutant, indicating that the observed oxygen-associated Pchlide levels in different species are regulated by oxygen sensing (Fig. 1b, Extended Data Fig. 1b–d). In *A. thaliana* accession Col-0 (originally collected less than 100 m above sea level (a.s.l.)) grown at 48 m a.s.l. (pO_2 = 21.2 kPa), this decrease was largely abolished in the absence of all 5 ERFVII transcription factors (using the pentuple *related to apetala* (*rap*) and *hypoxia responsive erf* (*hre*) mutant[18] *rap2.12 rap2.2 rap2.3 hre1 hre2* (hereafter referred to as *erfVII*)) (Fig. 1c), demonstrating that oxygen sensing via ERFVIIs is required for this response. A Cys-to-Ala mutation (Cys2Ala) (which removes the Cys N-degron) in all ERFVIIs significantly reduced Pchlide levels in etiolated seedlings, similar to *prt6* seedlings (in which all ERFVIIs are stable) (Fig. 1d). Mutation of either *PRT6* or ERFVII genes led to opposite stable changed steady-state Pchlide levels (lower in *prt6*, higher in *erfVII*s); mutation of *RAP2.3* had the largest effect, indicating that all ERFVIIs contribute to this function and that *RAP2.3* may have a predominant role (Extended Data Fig. 2a, b). A *prt6 flu* double mutant showed high levels of Pchlide equivalent to those in the *flu* mutant, indicating that stabilized ERFVIIs act upstream of *FLU* (Extended Data Fig. 2c). Because hypoxia suppressed Pchlide levels, we analysed the role of ERFVIIs in regulating expression of genes encoding components of the inactivating complex—including *FLU*, *HEMA1*, *CHL27* and POR (which is encoded by three genes, two of which (*PORA* and *PORB*) are expressed in etiolated seedlings[19])—and *CHLM*, which encodes a chlorophyll synthesis enzyme previously shown to be regulated by oxygen sensing[18]. Accumulation of *FLU* transcripts was positively regulated by *ERFVII*s via *PRT6*, whereas *CHL27*, *PORA*, *PORB* and *CHLM* were negatively regulated, and *HEMA1* was not regulated, by this pathway (Extended Data Fig. 2d). The amount of *FLU* RNA increased strongly with increasing hypoxia, a response that was abolished in the *erfVII* mutant, whereas expression of tetrapyrrole synthesis genes showed the opposite trend (Fig. 1e, Extended Data Fig. 2e). Reflecting the transcript data, FLU protein levels were enhanced by hypoxia via ERFVIIs, whereas POR protein accumulation was repressed by hypoxia through ERFVIIs (Extended Data Fig. 2f). Oxygen-controlled repression of *FLU*-orthologous RNA accumulation was conserved in *S. lycopersicum* and *P. somniferum* (Fig. 1f).

In *A. thaliana*, the C-terminally haemagglutinin (HA)-tagged ERFVIIs HRE2 and RAP2.3 associated with the *FLU* gene in a region containing an evolutionarily-conserved ERFVII binding site[20], adjacent to the initiating ATG (similar binding was previously observed for HRE2 at the *FLU* locus during the response of light-grown seedlings to hypoxia[20]). HRE2–HA and RAP2.3–HA also showed differential binding to two genes (*PCO1* and *CRU1*) previously shown to be regulated by ERFVIIs. HRE2 similarly associated with ATG-proximal regions of *CHL27* and *CHLM* genes, and

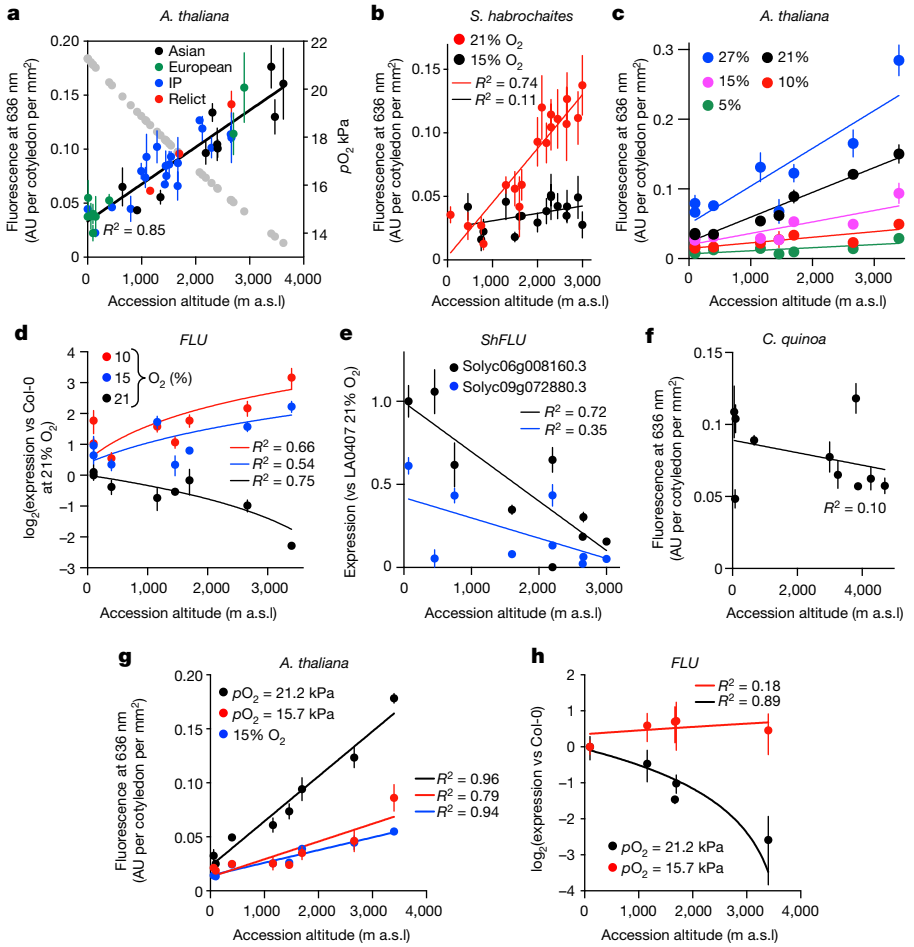

Fig. 2 | Steady-state levels of Pchlide and *FLU* expression are determined by altitude. a, Pchlide levels in *A. thaliana* accessions collected at different altitudes and geographic locations[30], grown at a pO_2 of 21.2 kPa. Grey dots show pO_2 at the different altitudes from which the accessions were collected. Genomic groups are indicated in different colours. IP, Iberian Peninsula **b**, Pchlide levels in *S. habrochaites* grown at 48 m a.s.l. with 21% and 15% ambient O_2. **c**, Effect of ambient O_2 concentration on Pchlide levels in *A. thaliana* accessions grown at 48 m a.s.l. (R^2 values from Supplementary Table 1b). **d**, **e**, Effect of ambient O_2 concentration on amount of *FLU* mRNA in *A. thaliana* (**d**) and *S. habrochaites* (**e**) grown at 48 m a.s.l. **f**, Pchlide levels in cultivated domesticated *C. quinoa* accessions obtained from different altitudes grown at pO_2 21.2 kPa. **g**, Comparison of Pchlide levels in *A. thaliana* accessions collected at different altitudes and grown at 48 m a.s.l. with pO_2 = 21.2 kPa or 15% ambient O_2, or at 2,479 m a.s.l.(pO_2 = 15.7 kPa). **h**, *FLU* RNA accumulation in *A. thaliana* accessions collected at different altitudes and grown at 48 m a.s.l. (pO_2 = 21.2 kPa) or at 2,479 m a.s.l. (pO_2 = 15.7 kPa). All experiments were carried out using etiolated seedlings after 5 days growth. Data are mean ± s.d. Accessions used are listed in Supplementary Table 1a. n = 3 biologically independent experiments.

also with gene regions of *PORA* and *PORB* but not with *HEMA1* (Fig. 1g, Extended Data Fig. 3). These data demonstrate that O_2 regulation of Pchlide synthesis occurs via oxygen sensing of the PCO N-degron pathway through ERFVII-regulated control of expression of components of the GluTR inactivation complex, in particular the negative regulator *FLU*.

Because pO_2 decreases with altitude (Fig. 2a), and could thus affect steady-state Pchlide levels, we investigated the relationship between Pchlide levels and altitude. We analysed Pchlide in accessions of *A. thaliana* (collected from Eurasia and Africa), *Solanum habrochaites* (collected from South America), *Solanum cheesmaniae* (collected from the Galapagos Islands) and *B. distachyon* (collected from Turkey) from natural populations growing at different altitudes from sea level to more than 3,000 m a.s.l. with different latitudinal ranges (Fig. 2a, b, Extended Data Fig. 4a, b, Supplementary Table 1a). When analysed at 48 m a.s.l. (pO_2 21.2 kPa), all species showed a positive correlation between altitude of accession collection and Pchlide steady state level. Furthermore, the amount of Pchlide in *A. thaliana* and *S. habrochaites* was dependent on the ambient O_2 concentration, and hypoxia resulted in greater reduction of Pchlide levels in accessions from higher altitudes (Fig. 2b, c). In *A. thaliana*, the steady-state Pchlide level was not related to submergence tolerance (Extended Data Fig. 4c, Supplementary Table 1c). As a result of increased Pchlide (which produces singlet oxygen[15] under light), following transfer to light, dark-grown seedlings of accessions collected at higher altitude accumulated substantially more reactive oxygen species (ROS) at 48 m a.s.l. than those collected at a lower altitude; this effect was dependent on the ambient O_2 level and functional *PRT6* (Extended Data Fig. 5). These results show that there is a relationship between Pchlide accumulation and the altitude of accession collection, suggesting adaptation of oxygen sensing and/or downstream signalling through the PCO N-degron pathway that fine-tunes steady-state Pchlide level to local atmospheric O_2 levels, potentially avoiding damaging light-associated singlet-oxygen ROS production. Consistent with such a relationship, we found that accumulation of *FLU* transcript in *A. thaliana* grown at 48 m a.s.l. (pO_2 = 21.2 kPa) was strongly influenced by the altitude at which the accession was collected (that is, there was less *FLU* transcript in high-altitude accessions) and by ambient O_2 level (Fig. 2d). There was a similar relationship between altitude of collection and *FLU* expression for *S. habrochaites* (*FLU* expression was lower in high-altitude accessions) (Fig. 2e). Conversely, the amounts of *PORA*, *PORB* and *CHLM* (but not *CHL27* or *HEMA1*) transcripts were higher in accessions from higher elevations, and lower at 15% oxygen compared with those grown in 21% oxygen (Extended Data Fig. 6a). POR protein accumulated to higher levels in the high-altitude *A. thaliana* accession Sha (originally collected in Tajikistan at 3,400 m a.s.l, pO_2 = 13.9 kPa) than in the low-altitude Col-0, and by introgressing the *prt6-1* transfer-DNA insertion mutation from Col-0 through eight back-crosses into Sha (*prt6*^{Sha}), we showed that this increase was controlled through the oxygen-sensing pathway; conversely FLU protein accumulation was increased in *prt6*^{Sha} compared with Sha (Extended Data Fig. 6b). In contrast to the observed relationship between the steady-state Pchlide level and elevation in wild species, an altitudinal cline of cultivated *Chenopodium quinoa* (quinoa, recently domesticated in the high Andes[21]) did not show altitude-dependent Pchlide accumulation (Fig. 2f).

Reduced pO_2 is just one altitude-dependent parameter: others include atmospheric pressure. We therefore assessed steady-state Pchlide levels and *FLU* expression in etiolated seedlings at two sites located at extreme altitudes (site SB: 52.829809° N −1.249732° E, 48 m a.s.l., pO_2 = 21.2 kPa; and site ESPE: −0.312917° N −78.445157° E, 2,479 m a.s.l., pO_2 = 15.7 kPa) (Extended Data Fig. 7). The Pchlide level was much lower in the high-altitude accession Sha when it was grown at

the high-altitude site ESPE compared with the low-altitude site SB, whereas in the *erfVII* mutant Pchlide level remained similar at both sites (Extended Data Fig. 8a). Steady state levels of Pchlide in an *A. thaliana* altitudinal cline were reduced at ESPE, compared to SB at pO_2 21.2 kPa, and were similar to accumulation at SB in 15% ambient O_2 (Fig. 2g). The amount of *FLU* transcript was also increased in plants grown under ambient O_2 concentration at ESPE compared with SB, particularly in high-altitude accessions, and was similar to the amount of *FLU* transcript in plants grown at SB under 15% O_2 (Fig. 2d, h), whereas the amounts of *PORA*, *PORB* and *CHLM* transcripts were lower in the plants grown under atmospheric O_2 concentration at ESPE compared with SB (Extended Data Fig. 8b). These data demonstrate that O_2 is the major component sensed by altitudinal clines when controlling steady-state Pchlide levels. They also indicate that high-altitude populations have adapted to lower ambient O_2 through increased O_2 sensitivity, and that this has occurred in phylogenetically distant angiosperm species. Reduced accumulation of *FLU* transcripts in high-altitude accessions at pO_2 21.2 kPa further suggests that they exhibit lower ERFVII activity compared with low-altitude accessions. In summary, the sensitivity to O_2 determines downstream Pchlide level, which is tailored to the local ambient pO_2 via regulation of *FLU* expression mediated by ERFVIIs.

Since the analyses carried out at different altitudes showed that the sensitivity to atmospheric O_2—as indicated by accumulation of Pchlide and its regulatory component *FLU*—increases with altitude, we examined the expression of classical hypoxia-associated genes. The expression of *ADH1*, *PDC1*, *PGB1* and *SUS4* transcripts (members of the core 49 conserved hypoxia-induced genes[22] that are regulated by ERFVIIs through the PCO N-degron pathway[23]) was highly dependent on both the altitude of accession collection and ambient oxygen level in both *A. thaliana* and *S. habrochaites* (Fig. 3a, Extended Data Figs. 8c, d). This indicates that altitude adaptation is not restricted to Pchlide accumulation and is a central conserved feature of oxygen sensing in angiosperms. Furthermore, it suggests that—similar to *FLU* regulation—at high oxygen levels, ERFVIIs are more active in low-altitude accessions than in high-altitude accessions. We next tested whether ERFVIIs are active in etiolated seedlings of the low-altitude accession Col-0 at pO_2 21.2 kPa. Pchlide level in Col-0 was intermediate between those in *prt6* and *erfVII* mutants (Fig. 1d), indicating ERFVII repressive activity. Increasing PCO2 activity in Col-0 led to increased levels of Pchlide, suggesting that active ERFVIIs can be destabilized, but this over-accumulation was inhibited by removal of *PRT6* activity (Fig. 3b).

To understand the genetic mechanisms involved in altitude adaptation through oxygen sensing, we investigated the influence of components of the ERFVII–PCO N-degron pathway in the high-altitude *A. thaliana* accession Sha. We transformed wild-type and Cys2Ala stable versions of the Col-0 ERFVIIs RAP2.3 and HRE2 (expression driven by their own promoters) into Sha. In *prt6*^{Sha}, RAP2.3(Cys2Ala)-expressing Sha and HRE2(Cys2Ala)-expressing Sha (but not in Sha expressing wild-type Col-0 RAP2.3), *FLU*, *PORA* and *PORB* expression were markedly affected, resulting in reduced Pchlide (Fig. 3c, d). In addition, expression of hypoxia-related genes was enhanced in *prt6*^{Sha} and RAP2.3(Cys2Ala)-expressing Sha (Extended Data Fig. 9a, b). This indicates that constitutively stabilized ERFVIIs reduce Pchlide as effectively in Sha as in Col-0. Therefore, components downstream of stabilized ERFVIIs, including *FLU* function, are unaltered in Sha (as otherwise altering upstream components would not affect the high Pchlide level in Sha). Expression of components of the PCO branch of the PRT6 N-degron pathway were not significantly different between Col-0 and Sha, and the sequences of Col-0 and Sha *FLU* genes were identical (Extended Data Fig. 9c, d). Etiolated seedlings from Sha × *erfVII* reciprocal crosses showed low Pchlide steady-state levels, indicating that ERFVII activity (in repressing Pchlide levels) in Sha has the potential to be as strong as that in Col-0 (Extended Data Fig. 10). This result also suggests the presence of dominant repressor(s) of oxygen sensing in the low-altitude accession Col-0. We further analysed ERFVII activity in Col-0 and Sha

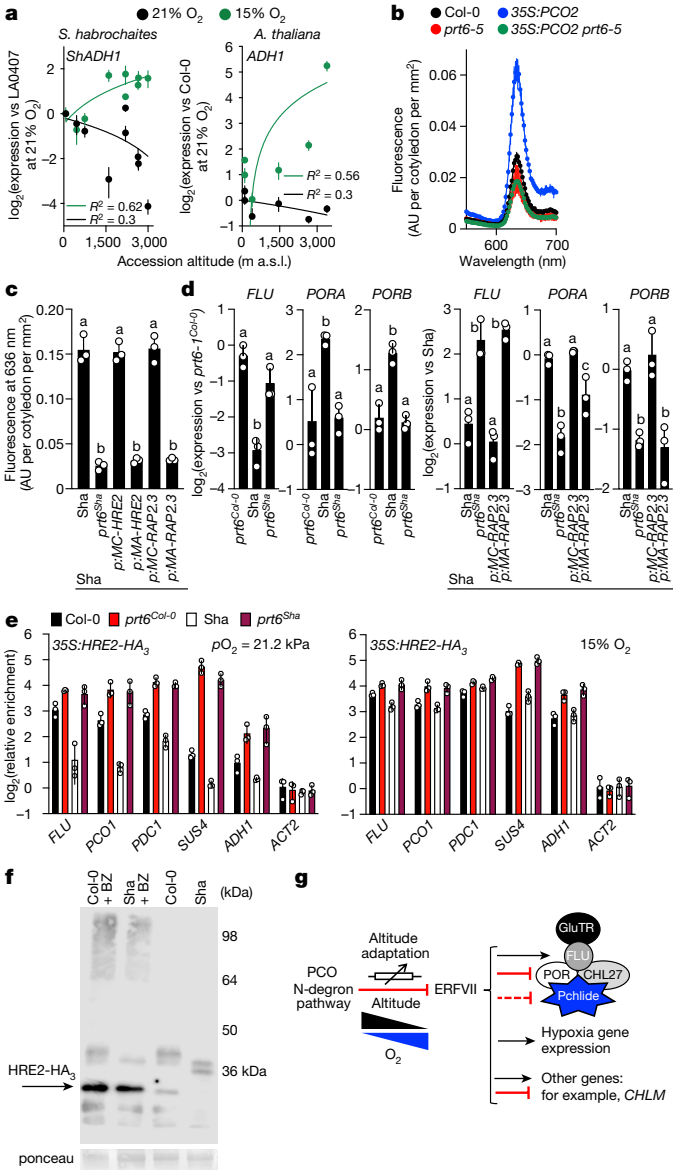

Fig. 3 | Genetic mechanisms linking oxygen sensing to altitude adaptation. **a**, Effect of ambient O_2 on RNA accumulation of hypoxia-associated *ADH1* in *S. habrochaites* and *A. thaliana* accessions. **b**, Pchlide levels in *prt6-5*, *35S:PCO2*, *prt6-5 35S:PCO2* and Col-0. **c**, **d**, Pchlide level and *FLU*, *PORA* and *PORB* transcript expression in *prt6-1* mutants and transgenic plants expressing wild-type or Cys2Ala mutant Col-0 RAP2.3 or HRE2 (driven by their own promoters) in Sha and Col-0 genetic backgrounds. **e**, ChIP analysis of HRE2–HA occupancy at *FLU* −49:+84 and hypoxia-related genes in Col-0 and Sha seedlings grown with pO_2 21.2 kPa or 15% ambient oxygen. **f**, Western blot analysis of HRE2–HA in Sha and Col-0 accessions grown at pO_2 21.2 kPa. The experiment was repeated independently three times with similar results. BZ, bortezomib. **g**, A model for angiosperm adaptation to altitude through oxygen sensing. Wedges indicate decreasing pO_2 with increasing altitude. Blocked arrows indicate repression. Arrow-crossed box is international standard symbol for a rheostat. The inactivation complex model is adapted from ref. [16]. All experiments were carried out using etiolated seedlings after 5 days growth at 48 m a.s.l. Data are mean ± s.d.; one-way ANOVA. Significantly different groups are indicated by letters in **c**, **d**. $n = 3$ biologically independent experiments.

by measuring HRE2–HA occupancy on *FLU* and hypoxia-related genes (which have been shown to bind HRE2 (ref. [20])). At a pO_2 of 21.2 kPa, HRE2–HA occupancy of these genes was high in the *prt6* mutant in both Sha and Col-0 backgrounds (in which HRE2 is stabilized), whereas in the wild type, HRE2–HA displayed lower occupancy of these genes in Sha than

in Col-0 (Fig. 3e). Occupancy increased in Sha and Col-0 when grown in 15% ambient O_2. Thus, at high ambient oxygen ERFVII occupancy is higher in the low-altitude genetic background, but HRE2 activity in both low- and high-altitude genetic backgrounds responds to hypoxia. Finally, Western blot analysis showed that at pO_2 21.2 kPa, HRE2–HA abundance was higher in Col-0 than in Sha, but treatment with the proteasome inhibitor bortizomib resulted in equivalent markedly higher HRE2–HA abundance in both accessions (Fig. 3f).

Here we demonstrate that altitude adaptation involves genetic modifications of the sensitivity to atmospheric O_2 through oxygen sensing, mediated by ERFVII accumulation and activity. We show that this adaptation, through ERFVII regulation, influences two distinct features: hypoxia-related gene expression and steady-state levels of Pchlide (mainly via oxygen-regulated expression of *FLU* and *POR*). Prevention of free Pchlide accumulation is a result of the regulated rate of ALA synthesis, mediated by the POR–Pchlide–CHL27 complex that triggers FLU inactivation of GluTR[24]. Coupling of *POR* expression to the ambient oxygen concentration may enable matching of POR protein to Pchlide levels, allowing POR to bind to free Pchlide. It may be ecologically important to match tetrapyrrole flux (which requires molecular O_2) to the ambient O_2 concentration to provide the most effective Pchlide level once seedlings arrive at the soil surface and chlorophyll synthesis commences in the light. Altitude adaptation involves fine-tuning the activity of the oxygen-sensing system, which acts like a rheostat measuring altitude (Fig. 3g), perhaps through negative regulation of the PCO N-degron pathway. Oxygen sensing is transduced by ERFVIIs to influence outputs including expression of hypoxia-related genes, steady-state Pchlide levels (through regulation of ALA synthesis by inactivation complex components) and potentially other biochemical pathways that require molecular oxygen. Altitude adaptation enables decoding of the ambient oxygen level (determined by the local pO_2) to provide equivalent outputs at different altitudes, resulting in, for example, equivalent Pchlide levels in a low-altitude (high pO_2)-adapted accession grown at low altitude to those in in a high-altitude (low pO_2)-adapted accession grown at high altitude.

Although this study only investigated etiolated seedlings, other stages of development (including analogous stages such as subsurface rhizome-derived etiolated shoots) may also be subject to a similar adaptive mechanism, as the steady-state Pchlide level is an important regulator of chlorophyll synthesis and FLU has been shown to influence the chlorophyll supply in light conditions[24]. Notably, regulation of tetrapyrrole synthesis by oxygen sensing also occurs in cyanobacteria, which share a common ancestor with chloroplasts[25]. Previous studies have shown that oxygen sensing is an important feature of skotomorphogenesis[18]. Here we demonstrate that oxygen sensing during this important developmental stage is associated with genetic adaptation to altitude. We show that local ambient absolute O_2 concentration regulates expression of hypoxia-related genes and steady-state levels of Pchlide—a biochemical intermediate of chlorophyll biosynthesis—in altitudinal clines of diverse species through the oxygen-sensing system. This provides a general mechanism for adaptation to absolute elevation that is likely to be conserved throughout angiosperms. In addition, as this mechanism appears to not have been selected in breeding of quinoa, it may represent an untapped trait for crop improvement at unadapted altitude[26]. It also represents a component that deserves investigation in relation to plant ecological adaptation. The relevance of this mechanism will be of increasing importance as global warming leads to displacement of wild and crop plants to higher altitudes[27].

Online content

Any methods, additional references, Nature Research reporting summaries, source data, extended data, supplementary information, acknowledgements, peer review information; details of author contributions and competing interests; and statements of data and code availability are available at https://doi.org/10.1038/s41586-022-04740-y.

1. Angel, R. et al. The root-associated microbial community of the world's highest growing vascular plants. *Microb. Ecol.* **72**, 394–406 (2016).
2. Dentant, C. The highest vascular plants on Earth. *Alp. Bot.* **128**, 97–106 (2018).
3. Brzezowski, P., Richter, A. S. & Grimm, B. Regulation and function of tetrapyrrole biosynthesis in plants and algae. *Biochim. Biophys. Acta* **1847**, 968–985 (2015).
4. Korner, C. The use of 'altitude' in ecological research. *Trends Ecol. Evol.* **22**, 569–574 (2007).
5. Bomblies, K. The high life: alpine dwarfism in *Arabidopsis*. *Plant Physiol.* **168**, 767 (2015).
6. Beall, C. M. Adaptation to high altitude: phenotypes and genotypes. *Annu. Rev. Anthropol.* **43**, 251–272 (2014).
7. Huerta-Sanchez, E. et al. Altitude adaptation in Tibetans caused by introgression of Denisovan-like DNA. *Nature* **512**, 194–197 (2014).
8. Lorenzo, F. R. et al. A genetic mechanism for Tibetan high-altitude adaptation. *Nat. Genet.* **46**, 951–956 (2014).
9. Holdsworth, M. J. & Gibbs, D. J. Comparative biology of oxygen sensing in plants and animals. *Curr. Biol.* **30**, R362–R369 (2020).
10. Gibbs, D. J. et al. Homeostatic response to hypoxia is regulated by the N-end rule pathway in plants. *Nature* **479**, 415–418 (2011).
11. Licausi, F. et al. Oxygen sensing in plants is mediated by an N-end rule pathway for protein destabilization. *Nature* **479**, 419–422 (2011).
12. Weits, D. A. et al. Plant cysteine oxidases control the oxygen-dependent branch of the N-end-rule pathway. *Nat. Commun.* **5**, 3425 (2014).
13. White, M. D. et al. Plant cysteine oxidases are dioxygenases that directly enable arginyl transferase-catalysed arginylation of N-end rule targets. *Nat. Commun.* **8**, 14690 (2017).
14. Schoefs, B. & Franck, F. Protochlorophyllide reduction: mechanisms and evolution. *Photochem. Photobiol.* **78**, 543–557 (2003).
15. Meskauskiene, R. et al. FLU: a negative regulator of chlorophyll biosynthesis in *Arabidopsis thaliana*. *Proc. Natl Acad. Sci. USA* **98**, 12826–12831 (2001).
16. Kauss, D., Bischof, S., Steiner, S., Apel, K. & Meskauskiene, R. FLU, a negative feedback regulator of tetrapyrrole biosynthesis, is physically linked to the final steps of the Mg^{++}-branch of this pathway. *FEBS Lett.* **586**, 211–216 (2012).
17. Hou, Z. W., Pang, X. Q., Hedtke, B. & Grimm, B. In vivo functional analysis of the structural domains of FLUORESCENT (FLU). *Plant J.* **107**, 360–376 (2021).
18. Abbas, M. et al. Oxygen sensing coordinates photomorphogenesis to facilitate seedling survival. *Curr. Biol.* **25**, 1483–1488 (2015).
19. Oosawa, N. et al. Identification and light-induced expression of a novel gene of NADPH-protochlorophyllide oxidoreductase isoform in *Arabidopsis thaliana*. *FEBS Lett.* **474**, 133–136 (2000).
20. Lee, T. A. & Bailey-Serres, J. Integrative analysis from the epigenome to translatome uncovers patterns of dominant nuclear regulation during transient stress. *Plant Cell* **31**, 2573–2595 (2019).
21. Jarvis, D. E. et al. The genome of *Chenopodium quinoa*. *Nature* **542**, 307–312 (2017).
22. Mustroph, A. et al. Cross-kingdom comparison of transcriptomic adjustments to low-oxygen stress highlights conserved and plant-specific responses. *Plant Physiol.* **152**, 1484–1500 (2010).
23. van Dongen, J. T. & Licausi, F. Oxygen sensing and signaling. *Annu. Rev. Plant Biol.* **66**, 345–367 (2015).
24. Hou, Z. W., Yang, Y. Y., Hedtke, B. & Grimm, B. Fluorescence in blue light (FLU) is involved in inactivation and localization of glutamyl-tRNA reductase during light exposure. *Plant J.* **97**, 517–529 (2019).
25. Ludwig, M. et al. ChlR protein of *Synechococcus* sp PCC 7002 is a transcription activator that uses an oxygen-sensitive 4Fe–4S cluster to control genes involved in pigment biosynthesis. *J. Biol. Chem.* **289**, 16624–16639 (2014).
26. Moat, J. et al. Resilience potential of the Ethiopian coffee sector under climate change. *Nat. Plants* **3**, 17081 (2017).
27. Lenoir, J., Gegout, J. C., Marquet, P. A., de Ruffray, P. & Brisse, H. A significant upward shift in plant species optimum elevation during the 20th century. *Science* **320**, 1768–1771 (2008).
28. Holdsworth, M. J., Vicente, J., Sharma, G., Abbas, M. & Zubrycka, A. The plant N-degron pathways of ubiquitin-mediated proteolysis. *J. Integr. Plant Biol.* **62**, 70–89 (2020).
29. Marin-de la Rosa, N. et al. Large-scale identification of gibberellin-related transcription factors defines group VII ETHYLENE RESPONSE FACTORS as functional DELLA partners. *Plant Physiol.* **166**, 1022–1032 (2014).
30. Alonso-Blanco, C. et al. 1,135 genomes reveal the global pattern of polymorphism in *Arabidopsis thaliana*. *Cell* **166**, 481–491 (2016).

Methods

No statistical methods were used to predetermine sample size. Experiments were not randomized. The investigators were not blinded to allocation during experiments and outcome assessment.

Plant materials

Information on *A. thaliana*, *S. habrochaites*, *S. cheesmaniae*, *B. distachyon* *P. somniferum* and *C. quinoa* accessions (Supplementary Table 1): *A. thaliana* accessions were obtained from NASC, UK. The *A. thaliana* *prt6-1*, *–5*, *erfVII* and individual mutant *ERFVII* lines (all in Col-0 accession background) were described previously[18,31]. The *flu-1* (Col-0 background) mutant[32] was obtained from M. Terry. The *35S:PCO2-FLAG*[12] transgenic (Col-0 background) was obtained from F. Licausi. *Solanum* accessions were obtained from TGRC, UC Davis, USA. *C. quinoa* cultivated accessions and *B. distachyon* accessions were obtained from the US National Plant Germplasm Collection Germplasm Resources Information Network (GRIN), Beltsville, US Department of Agriculture, Agricultural Research Service (http://www.ars-grin.gov/), and the *B. distachyon* accession Bd21 was provided by L. Mur. *P. somniferum* ('Lauren's grape') seeds were obtained from Mr. Fothergill's seeds, UK, and tomato *Solanum lycopersicum* (Marmande) were obtained from Sutton Seeds, UK. The Col-0 accession *prt6-1* T-DNA insertion was introgressed through eight back-crosses into the Sha accession following BASTA resistance conferred by the transgene. The *35S:HRE2*-3×HA transgene[10] from Col-0 was introgressed into Sha through five back-crosses following BASTA resistance conferred by the transgene, genotyping across all five chromosomes was used to confirm absence of detectable Col-0 genomic DNA away from both transgenes.

Growth conditions for etiolated seedlings

As previously described[18], surface-sterilized seeds were plated on 0.5× MS media (including 1% w/v sucrose) and chilled for 4 days at 4 °C before being exposed to constant white light at 20 °C for 8 h to activate germination. Subsequently, unless indicated otherwise, plates were incubated in darkness at 20 °C for 5 days. For experiments using different oxygen levels, open plates were placed in a methacrylate chamber (1,120 × 180 × 270 mm) (Epica) and flushed until equilibrium with water-saturated premixed gas combinations (BOC) and left for 5 days in the dark. Oxygen levels in the chamber were measured at the beginning and end of the experiment using an oxygen meter attached to the outlet pipe (KANE 250 Compact Flue Gas Analyzer-Kane International).

Generation of transgenic plants

Individual C2A and WT ERFVII transgenes, including 2 kbp of sequence upstream of the initiating ATG and introns in accession Col-0 were described previously[18]. These were transformed into *A. thaliana* accession Sha as previously described[33].

Biochemical analyses

Measurements of Pchlide and ROS. Pchlide was assayed from cotyledons isolated from etiolated seedling as described[34]. Cotyledons (or whole coleoptiles of *B. distachyon*) of etiolated seedlings were homogenized in 1 ml ice-cold 80% (v/v) acetone overnight at 4 °C. Extractions were vortexed and centrifuged, 800 µl was aliquoted into a fresh tube and 200 µl was used to measure the relative fluorescence at room temperature (excitation: 440 nm; emission: 550–750 nm) using either a Varioskan Flash (Thermo Fisher Scientific) for measurements at SB, or BioTek Cytation 5 Multi-Mode Reader (for measurements at ESPE). To account for differences in cotyledon size between accessions, images of 20 representative cotyledons for each accession in each experiment were taken using a Leica MZ75 and the area was measured using Fiji (https://imagej.net/). Reported Pchlide values represent the florescence (either from 550 to 700 nm or at 636 mn (arbitrary units)) per cotyledon in a 1 mm^2 area.

ROS were detected in 5 days old etiolated seedlings 1 day after transfer to light, 10 µM 2′,7′-dichlorodihydrofluorescein diacetate (H_2DCFDA) was incubated with seedlings for 30 min and then washed in 10 mM MES, 0.1 mM $CaCl_2$, pH 6, for 1 h at 22 °C. Dye excitation was at 480 nm and emitted light was detected at 535–550 nm with a Leica DM5000 B. ROS and chlorophyll quantification was carried out using Fiji.

ChIP, gene expression and protein analyses. ChIP was performed as described[35]. Chromatin was extracted from ~3.5 g of etiolated seedlings. Ten microgrammes of anti-HA (Sigma, H3663-200UL) was used for immunoprecipitation. *EUKARYOTIC TRANSLATION INITIATION FACTOR 4A1* (*EIF4A1*, AT3G13920) and *ACTIN 2* (*ACT2*, AT3G18780) were used as negative targets. *CRUCIFERINA* (*CRU1*, AT5G44120) and *PLANT CYSTEINE OXIDASE 1* (*PCO1*, AT5G15120) served as a known positive targets for RAP2.3 and HRE2 (refs. [20,29]). Chromatin was purified using QIAquick PCR Purification Kit (Qiagen). Quantitative PCR values of the immunoprecipitation product were normalized against the no-antibody samples. Data presented shows the average of three independent biological repeats. Oligonucleotide primers for ChIP are listed in Supplementary Table 2. For quantitative real time (QrtPCR), RNA was extracted from etiolated seedlings using a RNeasy mini kit (Qiagen) and DNase I on-column digestion (Sigma). First strand cDNA was synthesized using a qScript cDNA Synthesis Kit (Quantabio) from 0.8 µg RNA. rtPCR was performed using PerfeCTa SYBR Green FastMix (Quantabio) and the BioRad CFX96 qPCR system. Relative values were normalized over housekeeping genes in the appropriate species. Data presented shows the average of three independent biological repeats. Oligonucleotide primers used for rtPCR are shown in Supplementary Table 2.

Western blots were carried out as previously described[36]. The mouse anti-HA antibody (Sigma-Aldrich) was used at a concentration of 1:1,000 dilution, anti-POR (Agrisera AS05 067-10) was used at 1:4,000 dilution, and anti-FLU (obtained from B. Grimm) was used at 1:2,000 and the secondary antibody, goat anti-mouse IgG1 horseradish peroxidase conjugate (Thermo Fisher Scientific) was used at 1:20,000 dilution. Proteins were extracted from 5-day-old etiolated seedlings under green light as previously described[37]. Bortizomib treatment was carried out in 6-well tissue culture plates (Fisher Scientific); a total reaction volume of 3 ml of 50 µM Bortezomib (Santa Cruz Biotechnology) was added to each well. Negative controls contained an equivalent volume of DMSO (Sigma-Aldrich) (DMSO was used to reconstitute the Bortezomib powder). Five-day-old etiolated seedlings were transferred to each well by laying the seedlings on top of the solution in each well gently ensuring that the roots of each seedlings were immersed in the reaction solution. The plate was covered with aluminium foil and placed on a flatbed shaker (60 rpm) for 2 h, after which material was dried with paper towel to remove excess water and frozen in liquid nitrogen immediately.

Phylogenetic analyses

Genomic DNA and CDS sequences for *FLU*, *CHLM* and hypoxia-related gene orthologues were obtained from KEGG: Kyoto Encyclopedia of Genes and Genomes (https://www.kegg.jp/kegg/). *FLU*, *CHLM* genomic sequences were searched manually for potential ERFVII binding sites and HRPE-like sequences[20].

Statistics

For experimental analysis of Pchlide and quantitative reverse transcription PCR, three independent replicates with different biological material are reported for each experiment. For ChIP, three independent replicates with different biological material were used per experiment. Each experiment was repeated at least twice. For analysis of ROS via staining and microscopy 8–15 seedlings were analysed and images taken for representative samples, experiment was repeated at least three times. In all cases measurements were taken from distinct samples. Differences in ROS content were tested by general linear model (GLM) with two factors (genotype and oxygen) with fixed effects. GLM tests were carried

out with SPSS v.27. All graphs were produced using Graphpad software (Version 8), also used to calculate standard deviation of the mean for all samples tested. Relationships between dependent and independent variables were assessed by linear regression analysis using standard parameters for coefficiency of determination (R^2) in Graphpad.

Reporting summary

Further information on research design is available in the Nature Research Reporting Summary linked to this paper.

Data availability

Full versions of all blots are provided in Supplementary Fig 1. Unique identifiers for genes from all species analysed are listed in the text. Where appropriate, seeds of accessions and transgenic lines are available from the corresponding author. Source data are provided with this paper.

31. Holman, T. J. et al. The N-end rule pathway promotes seed germination and establishment through removal of ABA sensitivity in *Arabidopsis*. *Proc. Natl Acad. Sci.* **106**, 4549–4554 (2009).
32. Wagner, D. et al. The genetic basis of singlet oxygen-induced stress responses of *Arabidopsis thaliana*. *Science* **306**, 1183–1185 (2004).
33. Clough, S. J. & Bent, A. F. Floral dip: a simplified method for *Agrobacterium*-mediated transformation of *Arabidopsis thaliana*. *Plant J.* **16**, 735–743 (1998).
34. Terry, M. J. & Kacprzak, S. M. in *Phytochromes: Methods and Protocols* (ed. Hiltbrunner, A.) 169–177 (Springer, 2019).
35. Song, L., Koga, Y. & Ecker, J. R. Profiling of transcription factor binding events by chromatin immunoprecipitation sequencing (ChIP-seq). *Curr. Protoc. Plant Biol.* **1**, 293–306 (2016).
36. Vicente, J. et al. The Cys-Arg/N-end rule pathway is a general sensor of abiotic stress in flowering plants. *Curr. Biol.* **27**, 3183–3190 (2017).
37. Gibbs, D. J. et al. Nitric oxide sensing in plants is mediated by proteolytic control of group VII ERF transcription factors. *Mol. Cell* **53**, 369–379 (2014).
38. Gasch, P. et al. Redundant ERF-VII transcription factors bind to an evolutionarily conserved *cis*-motif to regulate hypoxia-responsive gene expression in *Arabidopsis*. *Plant Cell* **28**, 160–180 (2016).
39. Vashisht, D. et al. Natural variation of submergence tolerance among *Arabidopsis thaliana* accessions. *New Phyt.* **190**, 299–310 (2011).

Acknowledgements *Solanum sp*. accessions were obtained from the UC Davis/C.M. Rick Tomato Genetics Resource Center maintained by the Department of Plant Sciences, University of California, Davis, USA; *A. thaliana* accessions were obtained from NASC, Nottingham, UK; and quinoa and *B. distachyon* altitudinal cline accessions were provided by the US Department of Agriculture's National Plant Germplasm System, Plant Introduction Research Station, Ames, Iowa, USA. We thank M. Baldeon and O. Barreiro for generous use of equipment; B. Grimm for FLU antibody; G. Miño for technical support; and N. Crout and M. Blazquez for many helpful discussions. The work was funded by a Marie Curie CASCADE fellowship (600181) to M.A. and a Leverhulme Trust Research Project Grant (RPG-2018-172) to M.J.H. and was supported by the Biotechnology and Biological Sciences Research Council (grant number BB/R002428/1) to M.J.H. C.A.-B. was funded by grant PID2019-104249GB-I00 from the Agencia Estatal de Investigación of Spain (AEI)/10.13039/501100011033.

Author contributions M.J.H., M.A., C.A.-B. and K.P. designed the experiments. M.J.H., M.A., G.S., C.D. and J.M. carried out the experiments. M.A., C.A.-B. and M.J.H. conducted statistical analyses. M.J.H. and C.A.-B. wrote the manuscript with inputs from all co-authors. All co-authors read and approved the submitted manuscript.

Competing interests The authors declare no competing interests.

Additional information

Supplementary information The online version contains supplementary material available at https://doi.org/10.1038/s41586-022-04740-y.

Correspondence and requests for materials should be addressed to Michael J. Holdsworth.

Peer review information *Nature* thanks Nico Dissmeyer, Bernhard Grimm, Margret Sauter and the other, anonymous reviewer(s) for their contribution to the peer review of this work.

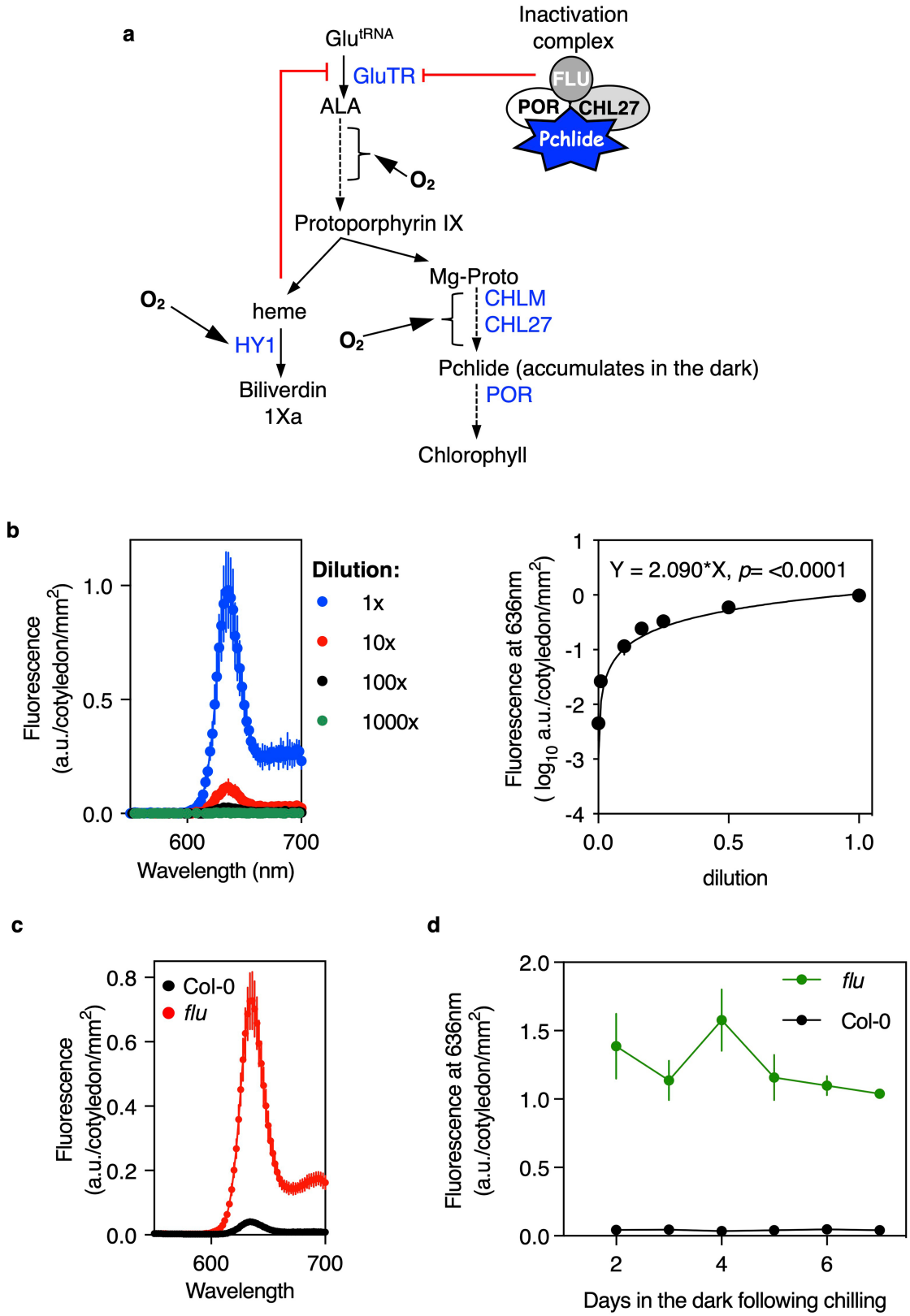

Extended Data Fig. 1 | See next page for caption.

Extended Data Fig. 1 | Tetrapyrrole synthesis and Pchlide steady state levels in etiolated seedlings. a, Schematic of tetrapyrrole synthesis showing points of oxygen requirement[3]. Blue, enzymes, black metabolites. Blocked arrows indicate repression. ALA, 5-aminolevulinic acid; Mg-Proto, Mg-protoporphyrin; GluTR, glutamyl-tRNA reductase; CHLM, MAGNESIUM-PROTOPORPHYRIN IX METHYLTRANSFERASE; HY1, HEME OXYGENASE1; POR, Light requiring PCHLIDE OXIDOREDUCTASE; FLU, FLOURESCENT IN BLUE LIGHT. Constituents of the GluTR inactivation complex are shown, diagram after[16]. b, Linearity of the measurement of Pchlide peak fluorescence at 636 nm, measured as arbitrary units (a.u.) per cotyledon per mm^2 (to account for differing cotyledon sizes between accessions of the same species), using the Pchlide over-accumulating Col-0 mutant *flu*. c, Pchlide levels in Col-0 (wild type) and *flu*. d, Levels of Pchide in *A. thaliana* during 7 days of etiolated growth of Col-0 (wild-type) and *flu*. Experiments carried out using etiolated seedlings after 5 days growth at pO_2 21.2 kPa (48 m a.s.l) unless otherwise stated. Means are plotted, error bars report SD. For each n = 3 biologically independent experiments.

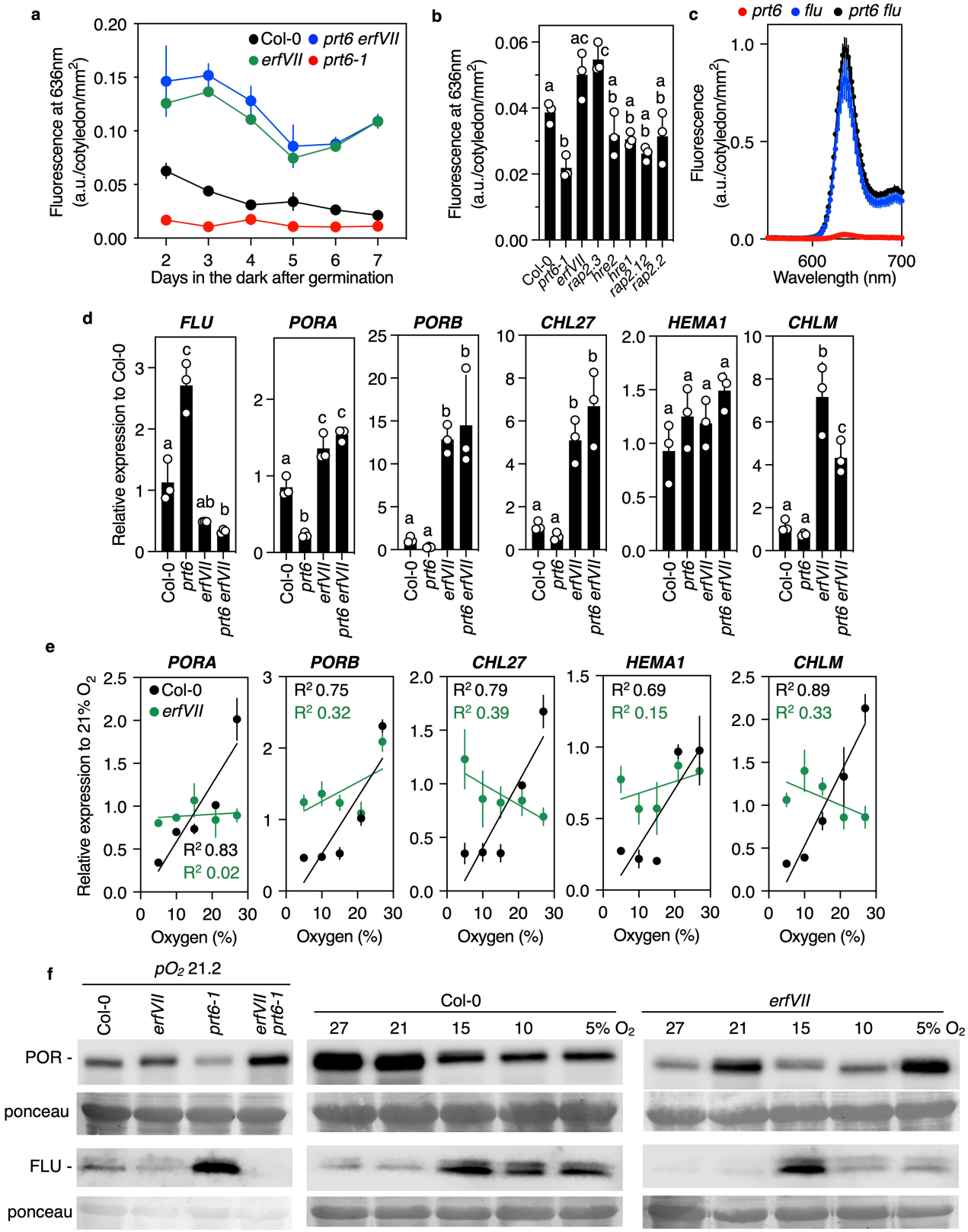

Extended Data Fig. 2 | See next page for caption.

Extended Data Fig. 2 | The influence of the PRT6 N-degron pathway and ERFVIIs on Pchlide levels. a, Pchide steady state levels in *A. thaliana* during 7 days of etiolated growth of Col-0 (wild-type) and N-degron pathway mutant *prt6-1* and *erfVII* combinations. b, Pchlide levels at pO_2 21.2 kPa (48 m a.s.l) in *A. thaliana* N-degron pathway mutant *prt6-1* and *erfVII* combinations and individual *ERFVII* mutants. c, Pchlide levels in *prt6*, *flu* and *prt6 flu*. d, Analysis of RNA expression of *FLU* and genes of tetrapyrrole synthesis in Col-0 (wild type) and *erfVII* and *prt6* mutants. e, Transcript levels in Col-0 and *erfVII* at different ambient oxygen levels. f, Accumulation of proteins for POR and FLU in Col-0 (wild type) and PRT6 N-degron pathway mutants at pO_2 21.2 kPa (48 m a.s.l), and in Col-0 and *erfVII* at different ambient oxygen levels, repeated independently three times with similar results. All experiments carried out using etiolated seedlings after 5 days growth at pO_2 21.2 kPa (48 m a.s.l) unless otherwise stated. Means are plotted, error bars report SD. Significant differences denoted with letters for one-way ANOVA ($p < 0.05$). Coefficient of determination (R^2) is given. For each n = 3 biologically independent experiments.

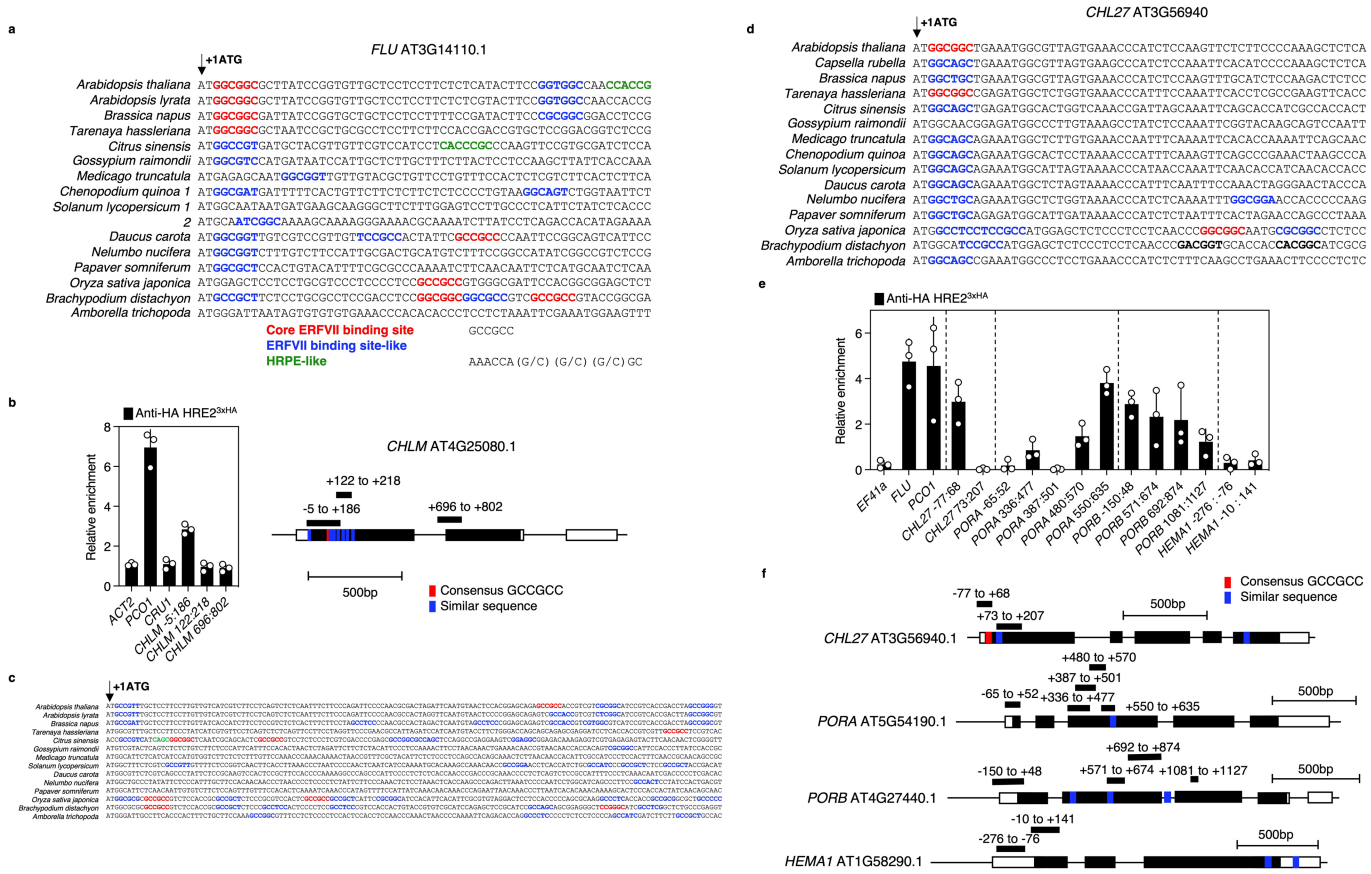

Extended Data Fig. 3 | ChIP analysis of HRE2 interaction with tetrapyrrole synthesis-related genes. a, Conservation of ERFVII binding site (also known as EBP, GC box) and related HRPE (Hypoxia-Responsive Promoter Element[38])-like element in the first coding exon of *A. thaliana FLU* and orthologues from selected angiosperms (initiating ATG highlighted). b, Schematic of the *CHLM* gene (repressed by ERFVIIs) showing ERFVII-binding sites and ChIP analysis of RAP2.3-3xHA and HRE2-3xHA occupancy of *CHLM* gene regions (including known positive and negative sequences[29]). c,d Conservation of ERFVII binding site in the first coding exons of *CHLM* and *CHL27* respectively. e, ChIP analysis of HRE2-3xHA occupancy of gene regions of *CHL27*, *PORA*, *PORB* and *HEMA1*. f, Schematics of genes showing positions of ERFVII and ERFVII-like binding sites. White boxes untranslated and black boxes translated regions. All experiments carried out using etiolated seedlings after 5 days growth at pO_2 21.2 kPa (48 m a.s.l). Means are plotted, error bars report SD. For each n = 3 biologically independent experiments.

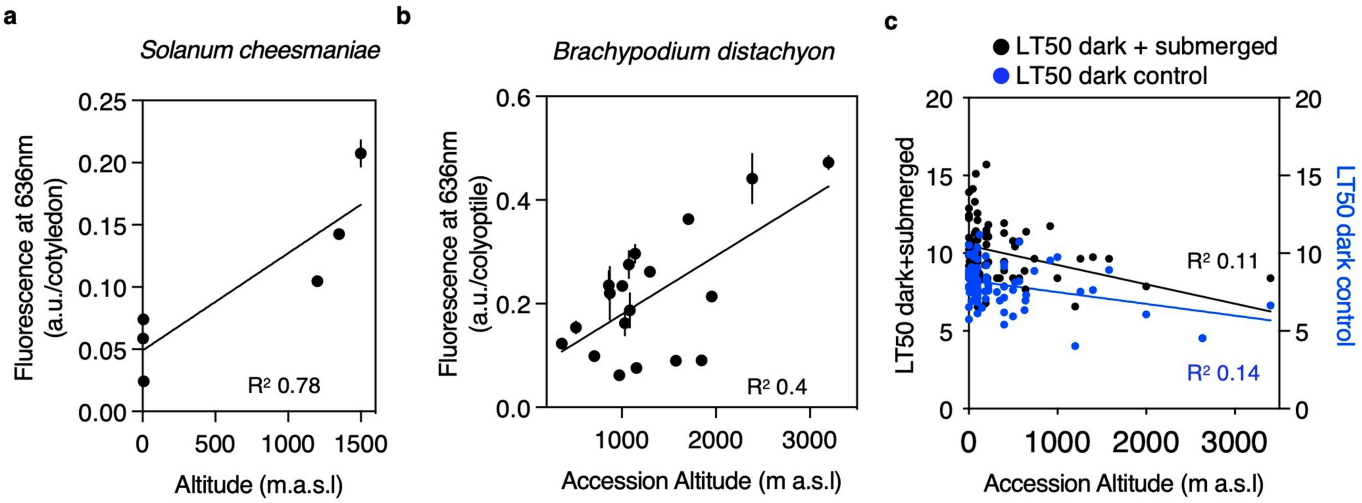

Extended Data Fig. 4 | Pchlide steady state levels and submergence tolerance for species accessions used in this study. a, b, Pchlide levels at pO_2 21.2 kPa in *S. cheesmaniae* and *B. distachyon* accessions collected at different altitudes and geographic locations. c, Relationship between *A. thaliana* accession and submergence tolerance, LT50 is defined as the number of days after which 50% of the plant population (for a particular accession) dies and was calculated from survival curves for each accession (data replotted from[39]), original data in Supplementary Table 1c. Coefficient of determination (R^2) is given. Means are plotted, error bars report SD. For each n = 3 biologically independent experiments.

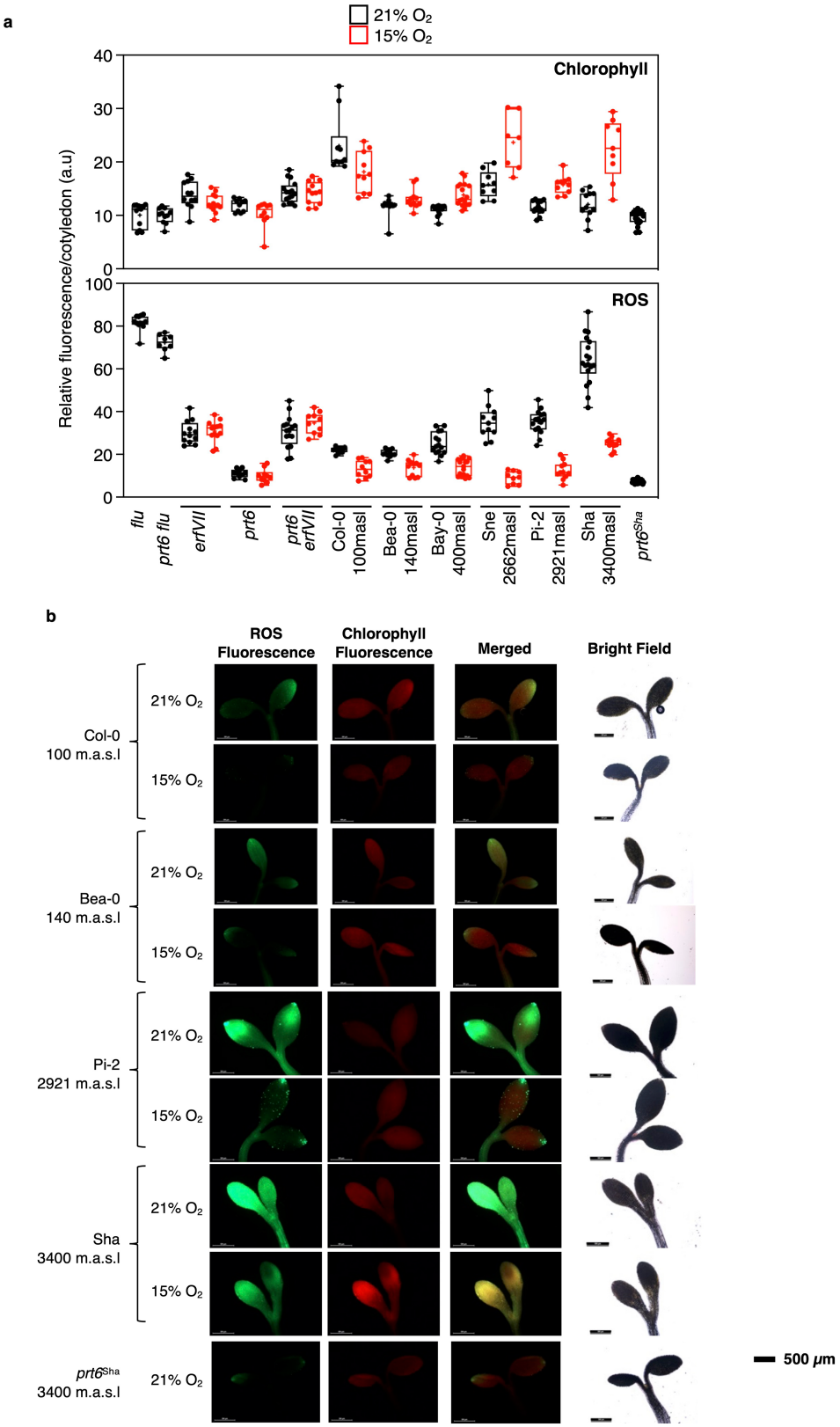

Extended Data Fig. 5 | ROS and chlorophyll accumulation in 5 day old etiolated seedlings after one day of light in *A. thaliana*. a. Relative fluorescence of ROS and chlorophyll. b. Example images of fluorescence of ROS and chlorophyll in different accessions at 21% and 15% ambient oxygen. Differences in ROS content were tested by GLM (General Linear Model) with two factors (Genotype and Oxygen) with fixed effects, both factors as well as the interaction where highly significant (Supplementary Table 1d). At least 8 seedlings were measured per accession, representative cotyledons are shown. For box and whisker plots whiskers go down to the minimum and up to the maximum values, boxes represent from 25th to 75th percentile and bars equal the median values.

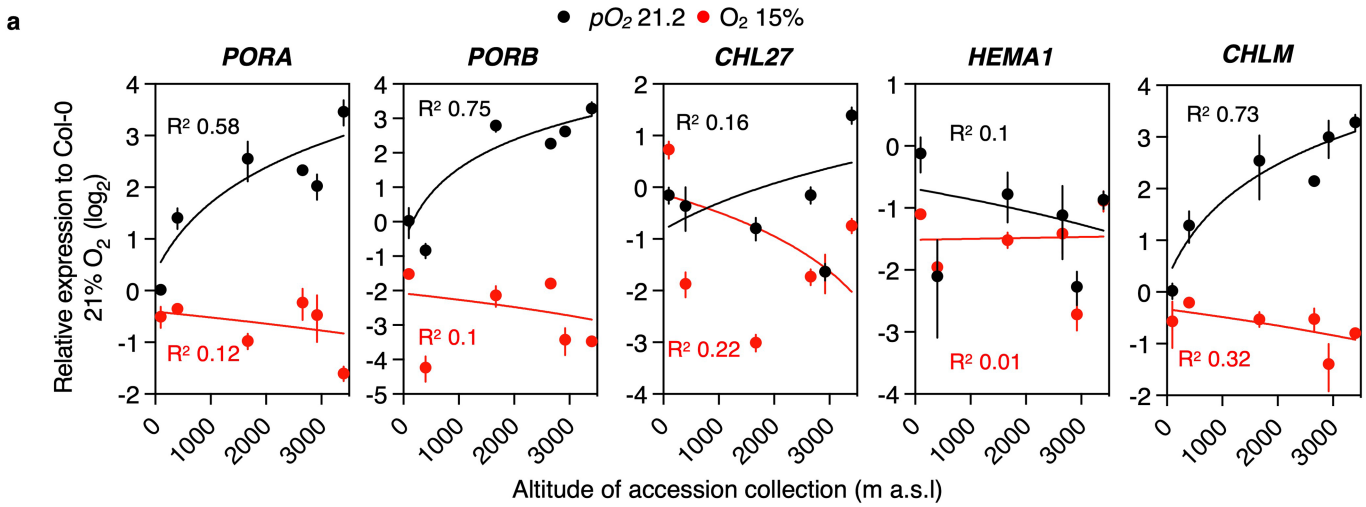

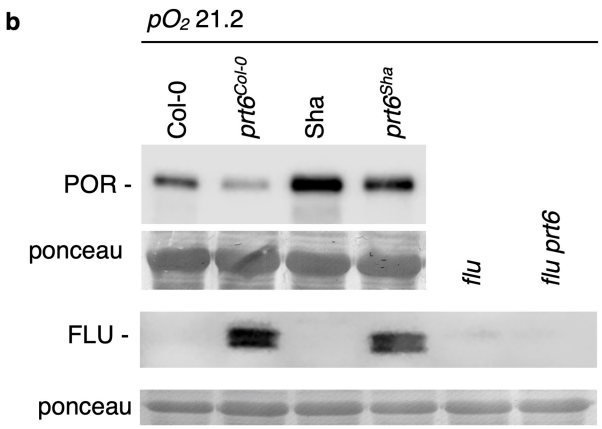

Extended Data Fig. 6 | Expression of RNA and protein for FLU, CHLM, HEMA1 and PORs in *A. thaliana* accessions. a, Analysis of RNA expression in accessions collected at increasing altitude at pO_2 21.2 kPa and 15% ambient oxygen. b, Accumulation of proteins for POR and FLU in Col-0 (wild type) and Sha, *prt6* (Col-0 background) and Sha *prt6*, repeated independently three times with similar results. All experiments were carried out using etiolated seedlings after 5 days growth at 48 m a.s.l unless otherwise stated. Means are plotted, error bars report SD. Coefficient of determination (R^2) is given. For each n = 3 biologically independent experiments.

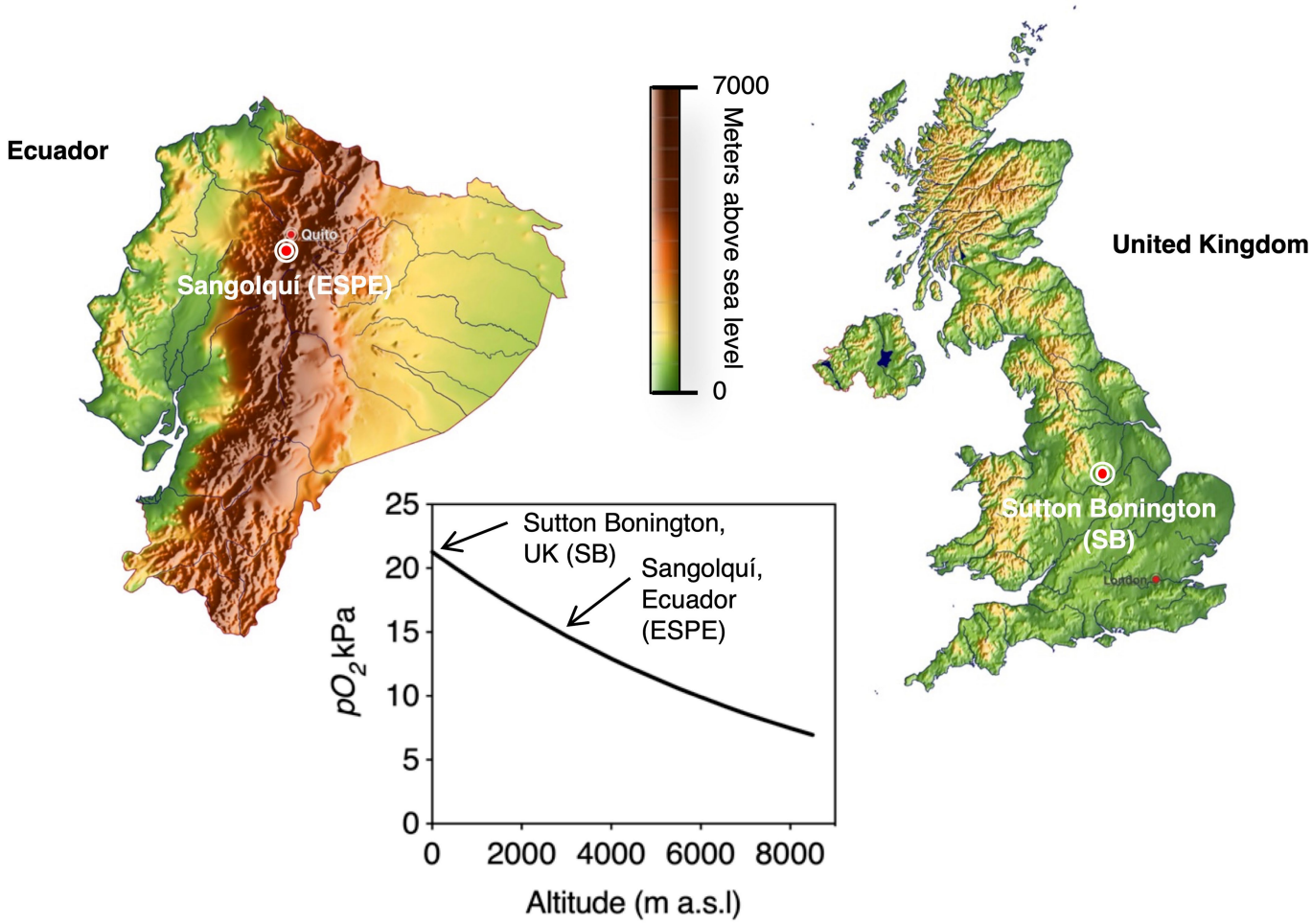

Extended Data Fig. 7 | Locations of sites used for reciprocal transplantation experiments. Relationship between altitude and partial pressure of oxygen (pO_2 kPa), showing positions of sites Sutton Bonington (SB): Latitude 52.829809° N longitude −1.249732° E pO_2 21.2 kPa: 48 m a.s.l, and Sangolquí (ESPE): Latitude −0.312917° N longitude −78.445157° E pO_2 15.7 kPa: 2479 m a.s.l. Maps obtained from http://www.ginkgomaps.com/.

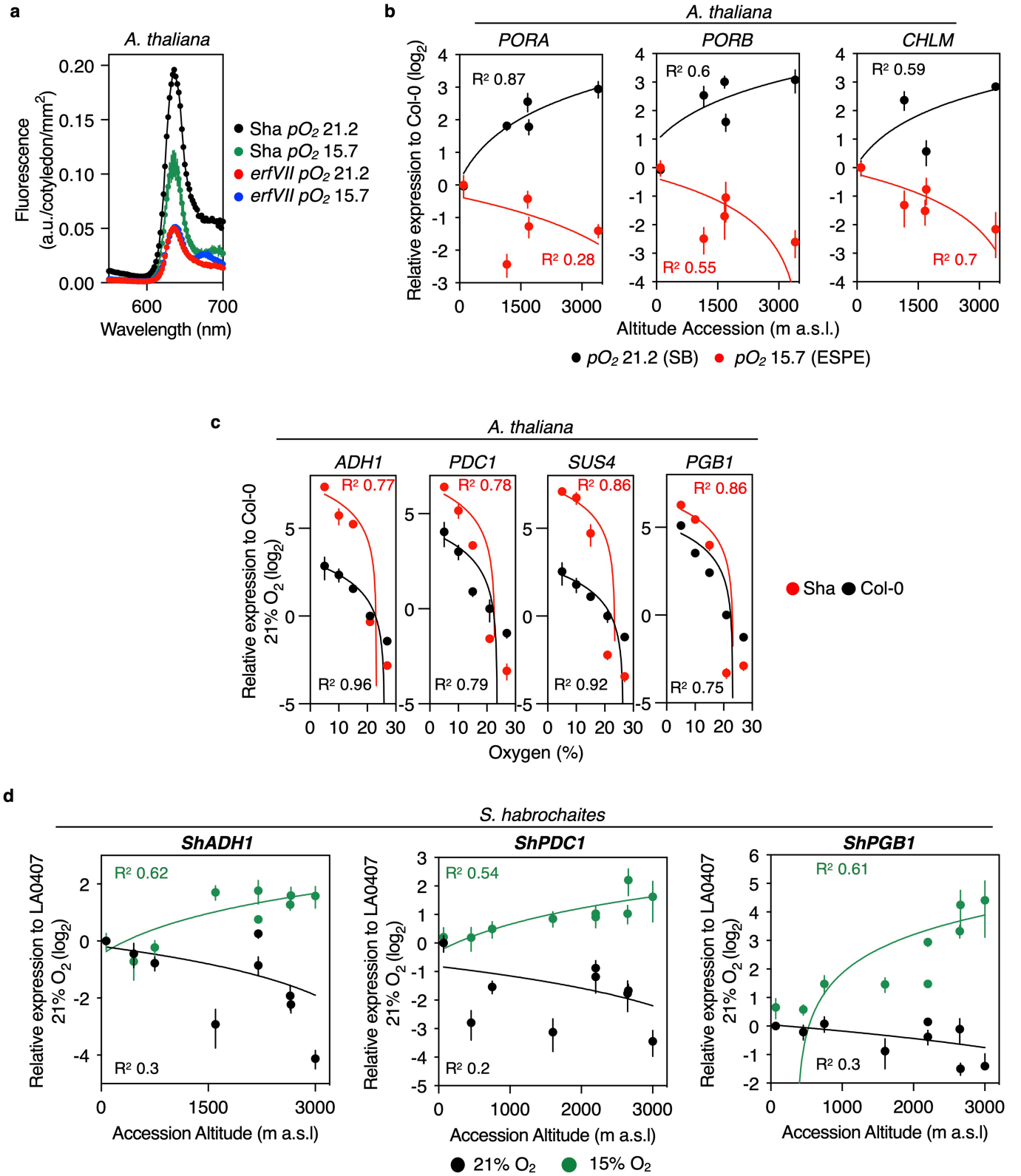

Extended Data Fig. 8 | Influence of ambient O_2 on expression of hypoxia-induced RNAs in *A. thaliana* and *S. habrochaites* accessions. a, Pchlide in *A. thaliana* high-altitude accession Sha, and *erfVII* (pentuple mutant obtained from the low altitude accession Col-0), measured at 48 m a.s.l. (SB, pO_2 21.2 kPa) and 2479 m a.s.l. (ESPE, pO_2 15.7 kPa). b, *PORA/B*, *CHLM* gene expression in *A. thaliana* accessions collected at different altitudes measured at 48 m a.s.l. (pO_2 21.2 kPa, SB) or at 2479 m a.s.l. (pO_2 15.7 kPa, ESPE). c, Hypoxia-related gene expression in *A. thaliana* accessions Col-0 (low altitude) and Sha (high altitude), at 48 m a.s.l. in different ambient levels of oxygen. d, Expression of *S. habrochaites* hypoxia-related genes at 15% and 21% ambient oxygen in accessions from different altitudes measured at 48 m a.s.l. Carried out using etiolated seedlings after 5 days growth (48 m a.s.l). Means are plotted, error bars report SD, coefficient of determination (R^2) is given. For each n = 3 biologically independent experiments. For a, Sha (SB) was measured once.

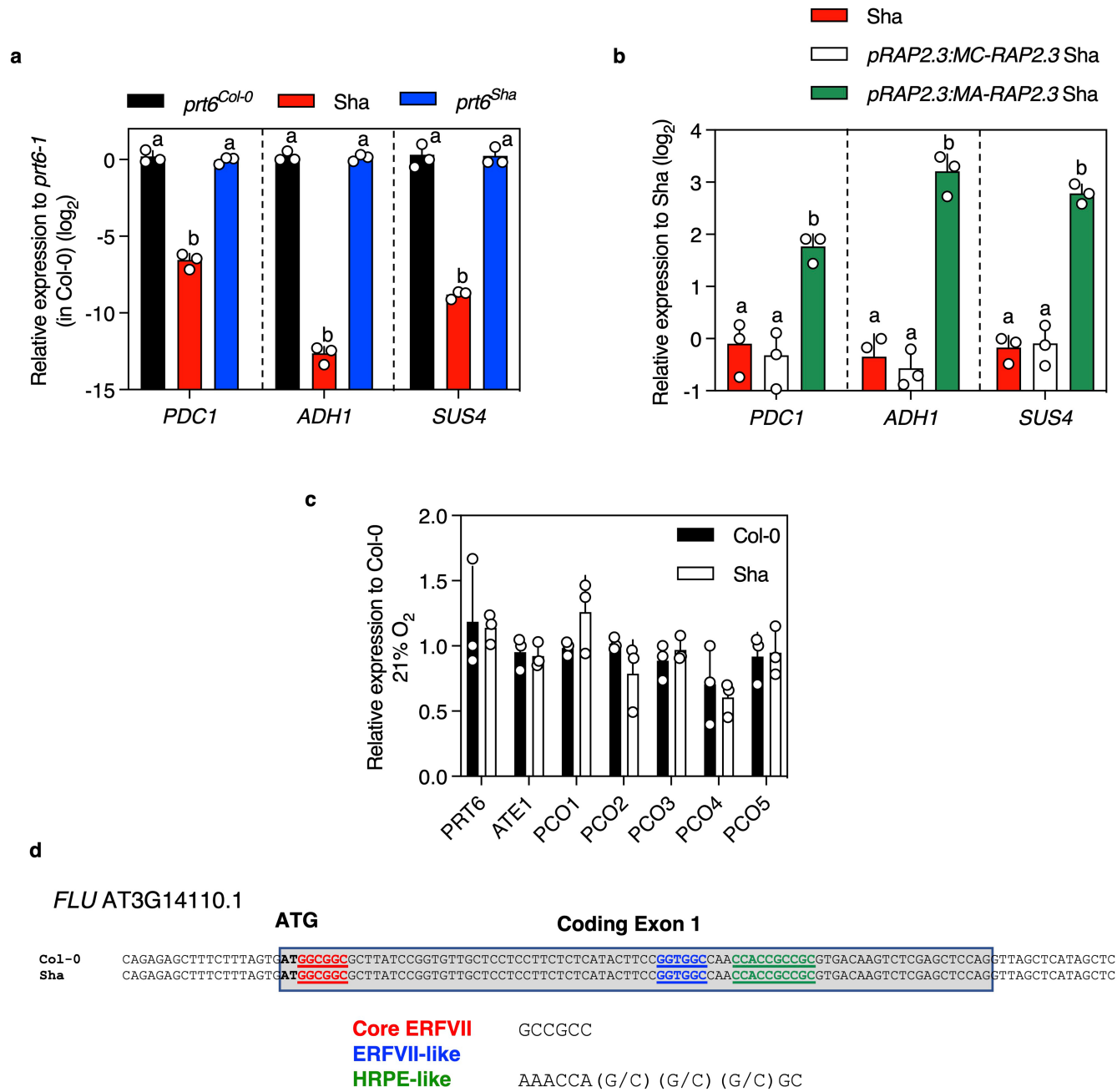

Extended Data Fig. 9 | Comparisons of genomic DNA and RNA expression patterns in *A. thaliana* accessions Col-0 and Sha. a,b Introduction of the *prt6-1* mutation (by introgression from low altitude accession Col-0) or C2A-RAP2.3 (by transformation) into *A. thaliana* high altitude accession Sha enhances the expression of hypoxia-related genes. c, Expression of RNAs for PCO PRT6 N-degron pathway components in accessions Sha and Col-0. RNA was extracted using etiolated seedlings after 5 days growth at pO_2 21.2 kPa (48 m a.s.l). d, Comparison of DNA sequence of the first coding exon of *FLU* in accessions Col-0 and Sha. DNA sequence information was obtained from Arabidopsis 1001 web site: http://signal.salk.edu/atg1001/2.0/gebrowser.php. Shown are ERFVII binding site (also known as EBP, GCC box) and related HRPE (Hypoxia-Responsive Promoter Element[2])-like element in the first coding exon of *A. thaliana FLU* (initiating ATG highlighted). All experiments carried out using etiolated seedlings after 5 days growth. Means are plotted, error bars report SD. Significant differences denoted with letters for one-way ANOVA ($p < 0.05$). For each n = 3 biologically independent experiments.

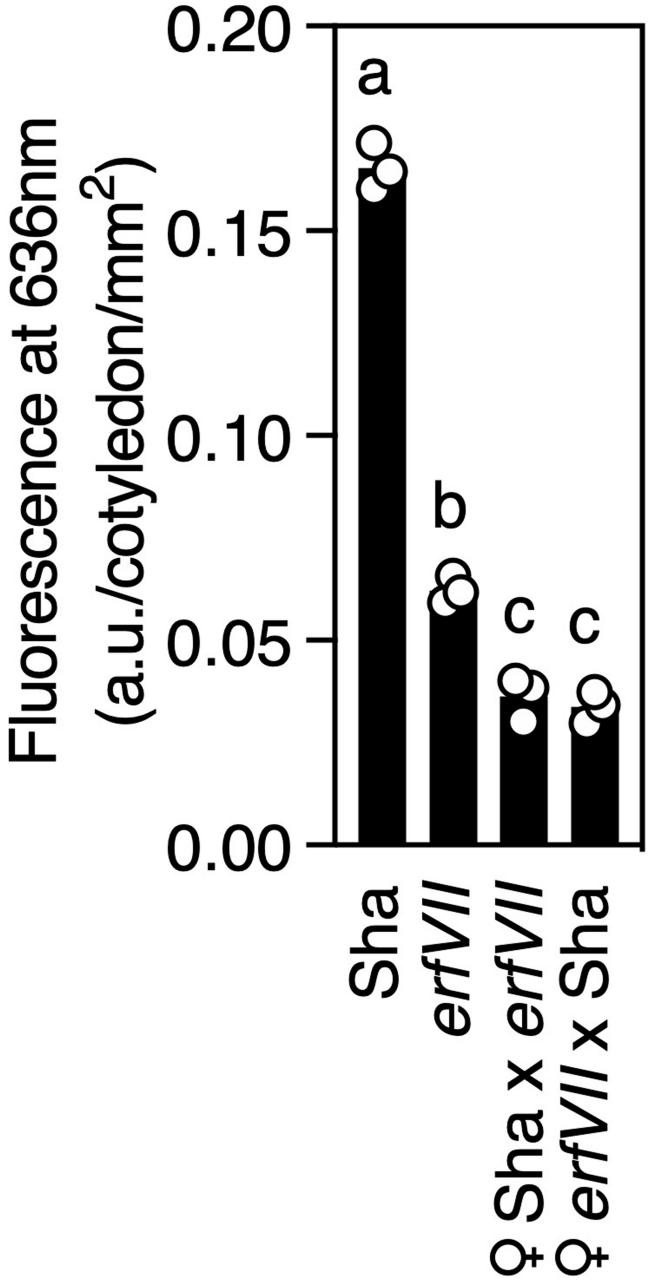

Extended Data Fig. 10 | Pchlide steady state levels in reciprocal genetic crosses between *A. thaliana* high altitude accession Sha and *erfVII* (Col-0 accession). Experiments carried out using etiolated seedlings after 5 days growth at pO_2 21.2 kPa (48 m a.s.l). Means are plotted, error bars report SD. Significant differences denoted with letters for one-way ANOVA ($p < 0.05$). For each n = 3 biologically independent experiments.

nature research

Corresponding author(s): Holdsworth

Last updated by author(s): Mar 3, 2022

Reporting Summary

Nature Research wishes to improve the reproducibility of the work that we publish. This form provides structure for consistency and transparency in reporting. For further information on Nature Research policies, see our Editorial Policies and the Editorial Policy Checklist.

Statistics

For all statistical analyses, confirm that the following items are present in the figure legend, table legend, main text, or Methods section.

n/a	Confirmed	
☐	☒	The exact sample size (*n*) for each experimental group/condition, given as a discrete number and unit of measurement
☐	☒	A statement on whether measurements were taken from distinct samples or whether the same sample was measured repeatedly
☐	☒	The statistical test(s) used AND whether they are one- or two-sided *Only common tests should be described solely by name; describe more complex techniques in the Methods section.*
☒	☐	A description of all covariates tested
☐	☒	A description of any assumptions or corrections, such as tests of normality and adjustment for multiple comparisons
☐	☒	A full description of the statistical parameters including central tendency (e.g. means) or other basic estimates (e.g. regression coefficient) AND variation (e.g. standard deviation) or associated estimates of uncertainty (e.g. confidence intervals)
☐	☒	For null hypothesis testing, the test statistic (e.g. *F*, *t*, *r*) with confidence intervals, effect sizes, degrees of freedom and *P* value noted *Give P values as exact values whenever suitable.*
☒	☐	For Bayesian analysis, information on the choice of priors and Markov chain Monte Carlo settings
☒	☐	For hierarchical and complex designs, identification of the appropriate level for tests and full reporting of outcomes
☒	☐	Estimates of effect sizes (e.g. Cohen's *d*, Pearson's *r*), indicating how they were calculated

Our web collection on statistics for biologists contains articles on many of the points above.

Software and code

Policy information about availability of computer code

Data collection	KEGG: Kyoto Encyclopedia of Genes and Genomes (https://www.kegg.jp/kegg/), release 101
Data analysis	Prism Graphpad (v8), Microsoft Excel for Mac (v16), http://batchgeo.com/, BARheatmapper: http://bar.utoronto.ca/ntools/cgi-bin/ntools_heatmapper.cgi , BioVenn, ImageJ, GLM tests were carried out with SPSS (Statistical Package for the Social Sciences) v.27

For manuscripts utilizing custom algorithms or software that are central to the research but not yet described in published literature, software must be made available to editors and reviewers. We strongly encourage code deposition in a community repository (e.g. GitHub). See the Nature Research guidelines for submitting code & software for further information.

Data

Policy information about availability of data

All manuscripts must include a data availability statement. This statement should provide the following information, where applicable:

- Accession codes, unique identifiers, or web links for publicly available datasets
- A list of figures that have associated raw data
- A description of any restrictions on data availability

Numerical data used to generate graphs are provided as Source Data. Full versions of all blots are provided in SI Fig 1. The source data behind all graphs is provided as separate Microsoft Excel files. Unique identifiers for genes from all species analysed are listed in the text. Where appropriate seeds of accessions and transgenic lines are available from the corresponding author.

Field-specific reporting

Please select the one below that is the best fit for your research. If you are not sure, read the appropriate sections before making your selection.

☒ Life sciences ☐ Behavioural & social sciences ☐ Ecological, evolutionary & environmental sciences

For a reference copy of the document with all sections, see nature.com/documents/nr-reporting-summary-flat.pdf

Life sciences study design

All studies must disclose on these points even when the disclosure is negative.

Sample size	We used three independent biological samples size following standard practice in the field. For seedling survival analyses three populations were analyzed that consisted of either 20 or 15 seeds each.
Data exclusions	S. habrochaites accessions LA0407 and LA1721 were excluded from analysis of Pchlide levels at 15% oxygen because of a lack of seed material
Replication	Data were collected from at least three independent replications for each experiment, and replication was successful and showed comparable trends. Almost all experiments were also replicated at least twice (for a small number not enough seeds were available) with similar observations. For Extended Data Figure 8a Sha (SB) was carried out once, but this measurement is repeated many times throughout the manuscript with similar results.
Randomization	For phenotyping and expression analyses of different genetic materials (accessions of different species, mutants and transgenic lines), samples were assayed and processed randomly, within each environment. For experiments analysing etiolated seedlings the positions of agar plates containing seedlings within dark growth chambers was randomised. For ROS analyses, samples from different genotypes were also assayed randomly in each oxygen level, with no a priori group allocation. Covariates were not considered because, for each experiment, all samples were processed using the same protocol and growth chamber, with randomization of pots or plates.
Blinding	Investigators were not blinded because this was not deemed necessary for our study. Samples were collected according to the genotype and environment of plants, but genotypes at each environment were processed randomly (see section on randomization).

Reporting for specific materials, systems and methods

We require information from authors about some types of materials, experimental systems and methods used in many studies. Here, indicate whether each material, system or method listed is relevant to your study. If you are not sure if a list item applies to your research, read the appropriate section before selecting a response.

Materials & experimental systems

n/a	Involved in the study
☐	☒ Antibodies
☒	☐ Eukaryotic cell lines
☒	☐ Palaeontology and archaeology
☒	☐ Animals and other organisms
☒	☐ Human research participants
☒	☐ Clinical data
☒	☐ Dual use research of concern

Methods

n/a	Involved in the study
☒	☐ ChIP-seq
☒	☐ Flow cytometry
☒	☐ MRI-based neuroimaging

Antibodies

Antibodies used	For ChIP: Anti-HA (Sigma, H3663-200UL; 1:2500 dilution). For Western blots: Anti-HA (Sigma, H3663-200UL; 1:1000 dilution), Anti-POR (Agrisera AS05 067-10,1:4000 dilution; Anti-FLU (generated by Prof. Grimm, Humboldt-Universität zu Berlin, 1:2000 dilution); secondary antibody, Goat anti-Mouse IgG1, HRP from Thermo Fisher Scientific, PA1 74421, 1:20000 dilution).
Validation	Validation of the antibodies has been reported by the producers and in many refereed publications. According to the manufacturer (Agrisera) anti-POR has confirmed reactivity against POR from Arabidopsis thaliana, and has been used in previous studies, eg: Ha, J.-H., Lee, H.-J., Jung, J.-H. & Park, C.-M. Thermo-Induced Maintenance of Photo-oxidoreductases Underlies Plant Autotrophic Development. Developmental Cell 41, 170-179.e174, doi:https://doi.org/10.1016/j.devcel.2017.03.005 (2017). Anti-FLU antibody has been used in previous studies and has confirmed reactivity against FLU from Arabidopsis thaliana, eg: Hou, Z. W., Pang, X. Q., Hedtke, B. & Grimm, B. In vivo functional analysis of the structural domains of FLUORESCENT (FLU). Plant J. 107, 360-376, doi:10.1111/tpj.15293 (2021).